Quantitative Investigations of the Stimulated Raman Effect Using Subnanosecond Light Pulses

D. von der Linde, M. Maier, and W. Kaiser
Physik-Department der Technischen Hochschule München, Germany
(Received 15 August 1968)

Stimulated Raman emission of high conversion efficiency was observed in a traveling-wave system. Using laser pulses of shorter duration than the lifetime of the acoustic phonons, stimulated Brillouin scattering could be eliminated as a competing nonlinear process. Good quantitative agreement was found between existing theory (which was extended to real light beams) and experimental observations.

A. INTRODUCTION

During the past years extensive literature has been accumulated dealing with the stimulated Raman effect[1] in gases, liquids, and solids. In spite of these extensive studies, a quantitative analysis of the saturation range is still lacking for the simple traveling-wave situation. For instance, the conversion efficiency of laser into Raman light for most organic liquids was found[2] to be consistently below 10^{-1}, while – at the high powers used – much higher values were expected on theoretical grounds.[3,4] It has been recognized for some time that the occurrence of other competing nonlinear processes is responsible for the poor quantitative agreement[5,6,9] between theory and experiment. There are two nonlinear processes which appear frequently together with the stimulated Raman scattering (SRS): the self-focusing and self-trapping[5,10] of the incident laser beam, and the generation of stimulated Brillouin scattering.[6]

When an intense laser pulse traverses a liquid, self-focusing and self-trapping occurs (at the end of the cell) if a threshold power level of P_{th} is exceeded (e.g., approximately 20 kW has been measured[7,8] in CS_2). The value of P_{th} is frequently considerably below the magnitude necessary for the observation of stimulated Brillouin and Raman scattering.[5,9] The enhanced light intensity within the filament produces intense Raman emission,[10] but our limited knowledge of the light filaments (formation, duration, and intensity distribution) prevents a quantitative analysis of the generated stimulated Raman light. It should be noted that, in most cases, only part of the laser light is trapped in filaments.

Quantitative investigations of the stimulated Brillouin scattering (SBS) have clearly shown that the steady-state gain factors of liquids[11–14] are frequently one order of magnitude larger than the gain factors for SRS. It is not surprising, therefore, that SBS competes successfully with SRS in many substances. In fact, SRS is strongly suppressed or even extinguished during most of the laser pulse while laser light is quantitatively converted into Brillouin light.[12] It has been shown in recent investigations that a time approximately equal to the phonon life time τ_B is required for the steady-state gain factor of SBS to reach its full value.[13] For times smaller than τ_B, the generation of SBS is greatly reduced,[15] and SRS can freely develop.[16]

In this paper we wish to report on experimental investigations in CS_2 with very high incident laser intensities; stimulated Raman scattering was generated well in the saturation region, and as a result, Raman emission was observed over the whole cross section of the laser beam. In addition, the pulse duration of the incident light was short enough to inhibit the production of SBS. On the other hand, our pulses were sufficiently long to operate in the steady-state region of SRS. Under these conditions, our experimental observations are in excellent agreement with theoretical predictions for the stimulated Raman effect. In Sec. B the theoretical results of Shen and Bloembergen[4] will be briefly reviewed, and extended in such a way that a direct comparison with our experimental situation is made possible. In the following sections new experimental observations are reported, and finally, in Sec. G, the quantitative agreement between theory and experiment is discussed.

B. THEORY

When a light wave of frequency ω_L is incident on a Raman active medium, a small amount of energy ($\simeq 10^{-7}$/cm) is spontaneously scattered at a Stokes shifted frequency $\omega_{S1} = \omega_L - \omega_v$, where ω_v represents the Raman vibrational frequency under consideration. At very high intensities (> 10 MW/cm^2) stimulated Raman scattering (SRS) occurs, i.e., the Stokes wave is strongly amplified through nonlinear coupling with the laser wave. The energy transfer from the laser to the Stokes wave can become so large that the Stokes wave reaches intensity levels approaching those of the incident laser beam; the laser beam is depleted accordingly. If the Stokes wave is sufficiently powerful, it acts as a source for the amplification of a light wave at $\omega_{S2} = \omega_L - 2\omega_v$. This process might be iterated generating higher-order Stokes waves with frequencies ω_{S3}, ω_{S4}, etc.

Shen and Bloembergen[4] have presented a theory for SRS, and derived a set of coupled nonlinear differential equations which describes the interactions of the laser wave of intensity I_L with higher Stokes waves of intensity I_{S1}, I_{S2}, etc., all propagating in the z direction. Neglecting dispersion and assuming a wavelength independent extinction coefficient α_0, we can write

$$\frac{dI_L}{dz} = -g_0 I_{S1} I_L - \alpha_0 I_L$$

$$\frac{dI_{S1}}{dz} = +g_{S1}(I_{S1} I_L - I_{S1} I_{S2}) - \alpha_0 I_{S1} \qquad (1)$$

$$\frac{dI_{S2}}{dz} = +g_{S2}(I_{S2} I_{S1} - I_{S2} I_{S3}) - \alpha_0 I_{S2}, \text{ etc.}$$

The gain coefficients are $g_{Si} = g_0 \omega_{Si}/\omega_L$, where

$$g_0 = \frac{8\pi c \omega_L N}{\hbar \omega_{S1}^4 n^2 \Delta\tilde{\nu}} \frac{d\sigma}{d\Omega} \qquad (2)$$

with N the number of molecules per cm^3, $d\sigma/d\Omega$ the spontaneous scattering cross section for the Raman line under consideration and $\Delta\tilde{\nu}$ its width, n the index of refraction, and c the velocity of light in vacuum.

Eqs. (1) were derived under the following assumptions. First, the generation and interaction with anti-Stokes waves was neglected. Second, terms producing (phasematched) off-axis higher Stokes components were omitted. These assumptions are well fulfilled in our experimental system, where narrow laser and Stokes beams of small divergence provide very little gain for anti-Stokes and off-axis Stokes emission (occurring usually in cones of several degrees). In fact, the observed anti-Stokes emission was several orders of magnitude below the values of the on-axis Stokes waves. Third, plane waves of infinite lateral extent were assumed in Eqs. (1). Since in real experimental situations, the light beams have a finite cross section with a definite radial intensity distribution, we have extended the theory for a direct comparison with our experimental results. It is convenient to introduce dimensionless parameters

$$Z = z g_0 I_L(0), \quad \beta = \alpha_0/g_0 I_L(0), \qquad (3)$$

and $g_i = g_{Si}/g_0$.

With the laser transmission

$$K_L(Z) = I_L(Z)/I_L(0)$$

and the Stokes conversion efficiencies

$$K_{Si}(Z) = I_{Si}(Z)/I_L(0), \qquad (4)$$

Eqs. (1) have now the form

$$\frac{dK_L(Z)}{dZ} = -K_{S1}(Z) K_L(Z) - \beta K_L(Z)$$

$$\frac{dK_{S1}(Z)}{dZ} = g_1[K_{S1}(Z) K_L(Z) - K_{S1}(Z) K_{S2}(Z)] - \beta K_{S1}(Z) \qquad (5)$$

$$\frac{dK_{S2}(Z)}{dZ} = g_2[K_{S2}(Z) K_{S1}(Z) - K_{S2}(Z) K_{S3}(Z)] - \beta K_{S2}(Z), \text{ etc.}$$

In order to solve Eqs. (5), we require the initial conditions $K_{Si}(0)$. The $K_{S1}(0)$ and the initial conditions for the higher Stokes components were estimated from the spontaneous Raman scattering at ω_{S1} and from the zero-point fluctuations at ω_{Si}, respectively. A constant value of $K_{Si}(0) = 10^{-12}$ was used in our calculations for all Stokes components since a variation of $K_{Si}(0)$ by two orders of ten did not alter significantly our results in the saturation range.

Machine calculations were performed for CS_2, where the Raman frequency is $\omega_v = 1.24 \times 10^{14}$ sec^{-1} and the Raman gain coefficient is $g_0 = 0.01$ cm/MW. This latter value has been found in previous experiments,[8] and is in good agreement with that calculated from Eq. (2) using the following numbers[8,17,18]:

$$N = 10^{22} \text{ cm}^{-3}, \quad \omega_L = 2.7 \times 10^{15} \text{ sec}^{-1},$$

$$d\sigma/d\Omega = 3.7 \times 10^{-30} \text{ cm}^2, \quad \Delta\tilde{\nu} = 0.5 \text{ cm}^{-1}.$$

It can be seen from Eq. (3), that Z and β are functions of $I_L(0)$; i.e., Z is not the only parameter for the calculation of our intensity ratios K_L and K_{Si}. In Fig. 1, we present the results of our machine calculations (up to the fourth Stokes component) for the following two situations:

Fig. 1(a): The laser transmission K_L and the conversion efficiencies for the different Stokes waves K_{Si} are calculated for a constant incident laser intensity $I_L(0) = 300$ MW/cm^2 as a function of the cell length z (path length travelled by incident light). The broken and solid curves represent results for linear extinction coefficients $\alpha_0 = 10^{-4}$ cm^{-1} and $\alpha_0 = 3 \times 10^{-3}$ cm^{-1}, respectively.

Fig. 1(b): The values for K_L and K_{Si} are calculated for a constant cell length $z_0 = 30$ cm as a function of the incident laser intensity $I_L(0)$. The two sets of curves refer again to the linear extinction coefficients $\alpha_0 = 10^{-4}$ cm^{-1} (broken line) and $\alpha_0 = 3 \times 10^{-3}$ cm^{-1} (solid line).

It is seen from Figs. 1(a) and (b) that high conversion efficiencies are predicted for SRS. Disregarding linear losses, all the incident laser photons are converted into photons of first Stokes frequency ($\omega_{S1}/\omega_L = 0.95$) and subsequently into higher Stokes components. The effect of the linear losses as a function of distance is readily seen in Fig. 1(a). It should be noted that the two Figs. 1(a) and 1(b) have the same upper scale Z.

We now extend our calculations to consider more realistic light beams. Since the photoelectric detection systems provide us with power values P_L and P_{Si} for the laser and Stokes beams, respectively, we are interested in calculating the power ratios.[19]

$$R_j = P_j(Z)/P_L(0)$$

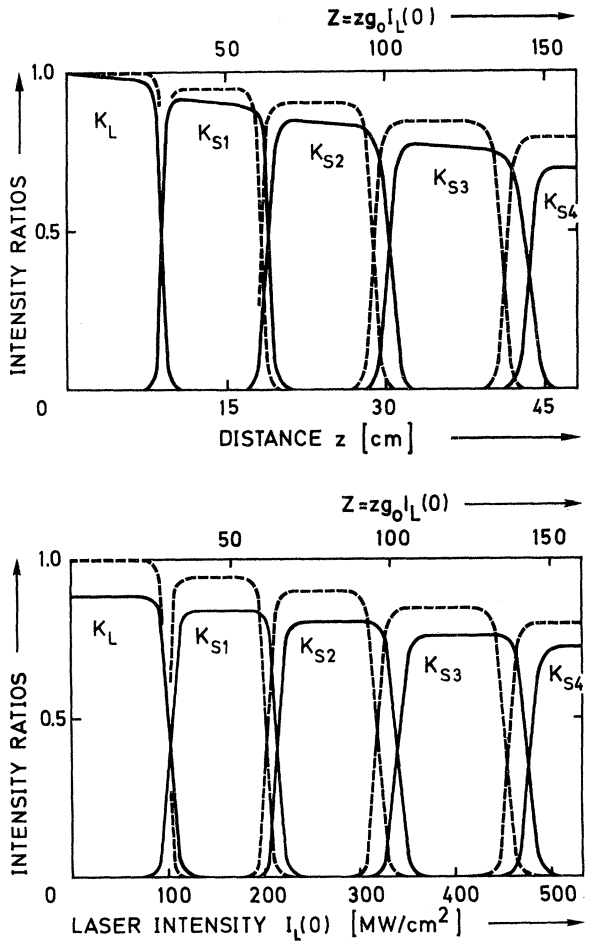

FIG. 1. Calculated intensity ratios of laser and Stokes light. Linear extinction coefficient $\alpha_0 = 3 \times 10^{-3}\ \mathrm{cm}^{-1}$ (solid curve) and $\alpha_0 = 10^{-4}\ \mathrm{cm}^{-1}$ (broken curve).
(a) Plane wave situation, constant incoming laser intensity $I_L(0) = 300\ \mathrm{MW/cm}^2$. Intensity ratios $K_L = I_L(z)/I_L(0)$, $K_{S1} = I_{S1}(z)/I_L(0)$, and $K_{S2} = I_{S2}(z)/I_L(0)$, etc., as a function of the distance z from the entrance window.
(b) Plane wave situation, constant cell length $z_0 = 30$ cm. The intensity ratios $K_L = I_L(z_0)/I_L(0)$, $K_{S1} = I_{S1}(z_0)/I_L(0)$, etc., as a function of the incident laser intensity $I_L(0)$. The upper scale in Fig. 1 (a) and Fig. 1(b) refers to the dimensionless variable $Z = zg_0 I_L(0)$.

$$= \frac{\int_0^\infty I_L(0,r) K_j[I_L(0,r)]\, r\,dr}{\int_0^\infty I_L(0,r)\, r\,dr}, \quad j = L, Si, \tag{6}$$

where r is the radial coordinate. With a Gaussian intensity distribution for the laser beam, entering the cell at position $z = 0$,

$$I_L(0,r) = I_L(0,0) \exp[-(r/r_0)^2] \tag{7}$$

and by changing the variable of integration, the power ratios can be rewritten

$$R_j = P_j(Z)/P_L(0)$$

$$= \frac{1}{I_L(0,0)} \int_0^{I_L(0,0)} K_j(I)\, dI, \quad j = L, Si\ . \tag{8}$$

The integrals rise (for all Si) to a maximum within the intensity range, where K_j has substantial values [see Fig. 1(b)]; for intensities beyond this range R_j is inversely proportional to $I_L(0,0)$. Using the solutions of K_j obtained for a cell length of $z_0 = 30$ cm, the power ratios R_j were calculated; they are plotted as a function of laser intensity $I_L(0,0)$ in Fig. 2. It is interesting to point out that for high laser intensities the strongly depleted laser and several Stokes components appear simultaneously at the exit window of the cell. This result is in contrast with the calculations of Fig. 1(b), where – after complete conversion – only one Stokes component (in the overlapping range at most two) is present in the Raman active medium. It will be shown in the subsequent sections that the experimental results agree very well with the calculated results depicted in Fig. 2.

C. EXPERIMENTAL

As light source for our investigations, a ruby laser (length of the crystal 7 cm) was used which was Q switched and mode locked by a cryptocyanine dye solution.[20] The output consisted of a train of light pulses, separated by a time $t_0 = 2l/c = 10$ nsec (corresponding to a length of the cavity of $l = 150$ cm). The duration of the pulses is determined by the number of modes coupled together. By using several resonant reflectors with different reflectivity characteristics as the front mirror, the pulse duration could be varied between approximately 0.5 and 3.0 nsec. These laser pulses have the advantage that their duration could be measured with a fast photoelectric detector and oscilloscope having an overall time constant of 0.3 nsec. The

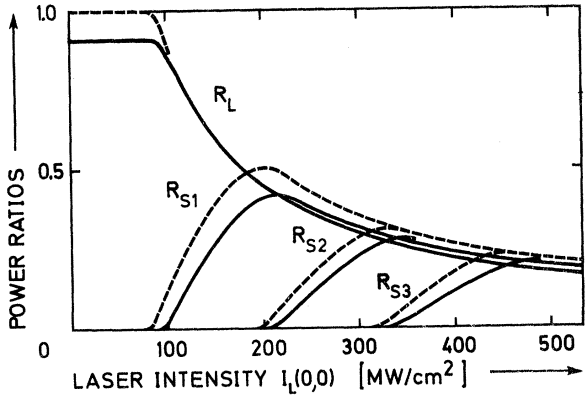

FIG. 2. Calculated power ratios $R_L = P_L(z_0)/P_L(0)$, $R_{S1} = P_{S1}(z_0)/P_L(0)$, R_{S2}, and R_{S3} as a function of the laser intensity $I_L(0,0)$ in the center of the Gaussian beam. $\alpha_0 = 3 \times 10^{-3}\ \mathrm{cm}^{-1}$ (solid curve), $\alpha_0 = 10^{-4}\ \mathrm{cm}^{-1}$ (broken curve), $z_0 = 30$ cm.

spectral width of the laser output measured with a high resolution Fabry-Perot interferometer was found to be consistent with the pulse duration measured with our fast photoelectric detectors.

A detailed investigation of the output beam, using a fast image converter camera, showed for each spike a smooth intensity distribution. With an integrating photographic plate, a Gaussian profile with a diameter of 0.15 cm (full width at $1/e$ points) and a beam divergence of 10^{-3} rad was measured.

With the same fast camera, we have studied the intensity distribution and the divergence of the Stokes beam. It was found from near field pictures that the Stokes emission extended over the whole cross section of the incoming beam. Frequently, a granular structure of the intensity distribution was observed, due to the presence of several bright filaments. With rising laser intensity, the intensity distribution of the Stokes beam became increasingly uniform, the bright spots disappearing in the intense over-all emission. The Stokes intensity profile was again approximately Gaussian with a diameter similar to that of the incoming beam. Measurements of the divergence of the Stokes beam gave for the full angle approximately 10^{-2} rad, a value which is also estimated from the geometry of the beam (length 30 cm and diameter 0.15 cm). This agreement was expected for the highly saturated Raman emission present in our experiments. We have measured the transmission of our CS_2 sample, and found α_0 values between 3 and 4×10^{-3} cm^{-1}. These linear losses result from scattering particles in our liquid.

The over-all accuracy of our data is estimated to be 20%, mainly due to uncertainties in the calibration of the photocells and the various filters, and to errors in the determination of the pulse heights on the oscilloscope traces.

D. TOTAL RAMAN CONVERSION EFFICIENCY AND LASER-PULSE DURATION

Very early during our investigations, a high conversion of laser into Raman light and a disappearance of SBS was observed when the pulse duration T decreased below 1 nsec. For a detailed analysis, an experimental system depicted schematically in Fig. 3 was used. With the help of two photocells (and using appropriate filters) the following four signals were measured simultaneously: the incoming laser power P_{IL},[19] the laser light transmitted by the liquid cell P_{TL}, the total stimulated Raman light generated in the forward direction P_R, and the Brillouin emission leaving the liquid in the backward direction P_B. The light beams P_{IL} and P_B were optically delayed by 4 nsec with respect to the signals P_{TL} and P_R in order to make two pulse trains observable on each oscilloscope. By properly triggering the two oscilloscopes, the corresponding pulses on the two traces were readily recognized. As an example, two oscilloscope pictures with together four-pulse trains are shown in Fig. 4. The following points should be noted: (a) For intense incoming pulses, the transmitted signals are substantially reduced,[21] suggesting a large conversion of laser light into

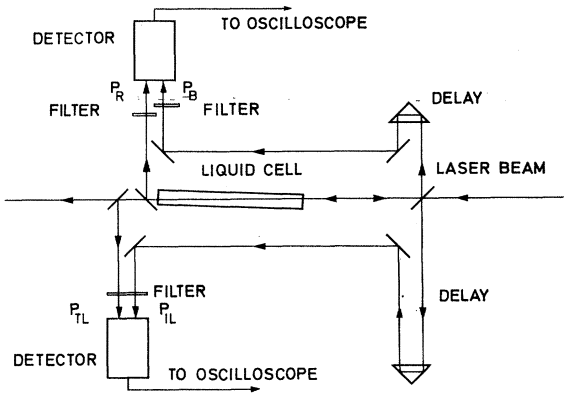

FIG. 3. Schematic of the experimental system for the investigation of stimulated Raman and Brillouin scattering. The laser beam enters from the right.

light of other frequencies and/or other directions. (b) Raman and Brillouin light (of high-power values) are only observed when the laser power exceeds a critical value, indicating a nonlinear process with a strong dependence on pump intensity. (c) The results of Fig. 4 were obtained with laser pulses of $T \simeq 2.0$ nsec (full width at half maximum intensity). For pulses with T between 0.6 and 1 nsec, no Brillouin signals P_B could be detected ($P_B/P_{IL} < 10^{-3}$).

In Fig. 5, the power ratios P_R/P_{IL} and P_B/P_{IL} are presented as a function of the pulse duration T. The peak values of the various pulses were used to evaluate P_R/P_{IL} and P_B/P_{IL}. The data were obtained for approximately the same value of incident laser power P_{IL}. It is clearly seen from Fig. 5 that for a pulse duration between 0.6 and 1.5 nsec, the Raman conversion efficiency is very large reaching values of $P_R/P_{IL} = 0.6$. With increasing pulse duration, the Raman conversion decreases quite drastically. It is interesting to see in Fig. 5 that the decrease of P_R/P_{IL} is accompanied by the appearance of strong Brillouin emission.

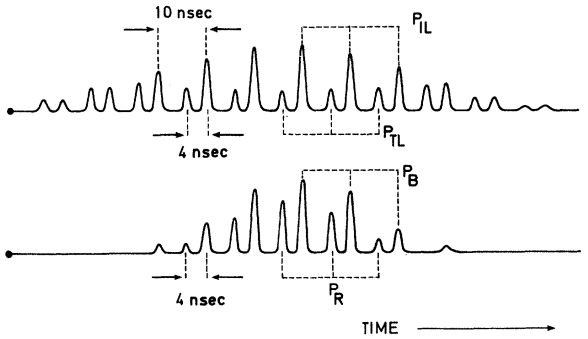

FIG. 4. Oscilloscope traces showing the incident and transmitted laser power P_{IL} and P_{TL} (upper trace) and the total Raman power P_R, and the Brillouin power P_B (lower trace).

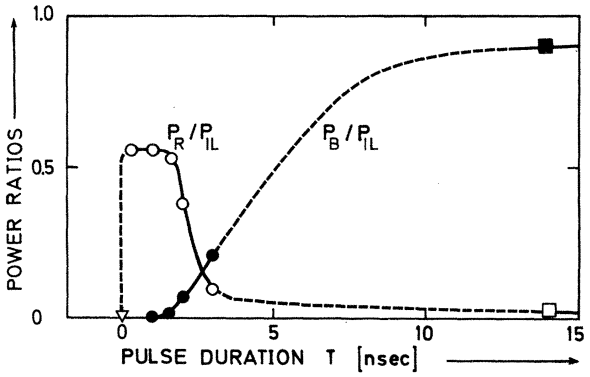

FIG. 5. Plot of the Raman (open symbols) and Brillouin (full symbols) conversion efficiencies as a function of the pulse duration T of the pump light. Circles: Conversion efficiencies obtained in the present investigation. For the other symbols see text. (There are no data in the range indicated by broken lines.)

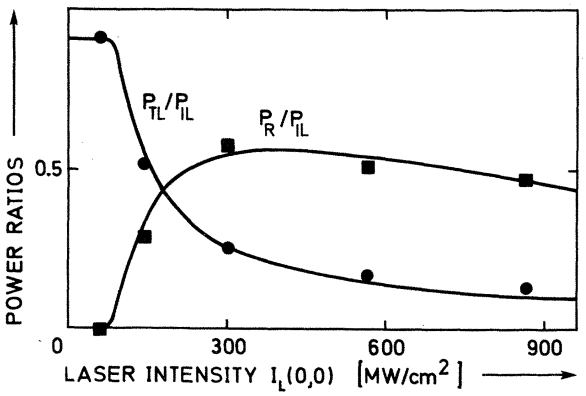

FIG. 6. Plot of the ratios transmitted laser power/incident laser power P_{TL}/P_{IL} and total Raman Stokes power/incident laser power P_R/P_{IL} as a function of the incident laser intensity $I_L(0,0)$. The circles and rectangles represent the experimental points. The solid curves were calculated for a Gaussian intensity distribution of the laser beam ($\alpha_0 = 3\times10^{-3}$ cm^{-1}).

At the right of Fig. 5, we have added results from previous investigations with conventional giant laser pulses of 14 nsec pulse duration.[12] For such pulses, a Brillouin conversion efficiency of 0.90 has been reported, while the Raman conversion – occurring in a short spike[8] prior to the development of the Brillouin emission – is rather small. We have, furthermore, included in Fig. 5 a point (triangle at the very left) taken from the literature,[16] where stimulated Raman scattering was investigated by very short light pulses of approximately 10^{-12} sec duration. For these light pulses, the gain constant for the stimulated Raman effect has not yet reached the steady-state value; in fact, a small power conversion of $P_R/P_{IL} < 4\times10^{-3}$ was reported.

We wish to conclude from the results depicted in Fig. 5 that for pulses with $0.6 < T < 1$ nsec, our investigations of SRS in CS_2 are not influenced by SBS. A steady-state theory for SRS appears to be appropriate.

E. TOTAL RAMAN CONVERSION EFFICIENCY AND LASER INTENSITY

With the experimental system discussed in Fig. 3, we measured the power ratios for the total Raman emission and for the transmitted laser light, P_R/P_{IL} and P_{TL}/P_{IL}, respectively, as a function of the incident laser power P_{IL}. Experimental data – obtained from pulse trains similar to those depicted in Fig. 4 – are presented in Fig. 6, where a pulse duration of 0.6 nsec and a cell length of 30 cm was used. The strong decrease of transmitted laser light, and the rapid increase in Raman power is quite apparent from Fig. 6. It should be emphasized that P_R includes the emission of all the Stokes-shifted Raman light, i.e., $P_R = \sum_i P_{Si}$. The lines drawn through our experimental points are obtained from computer calculations discussed in Sec. B; the following parameters, appropriate for our experimental system, were used: $g_0 = 10^{-2}$ cm/MW, $z_0 = 30$ cm and $\alpha_0 = 3\times10^{-3}$ cm^{-1}. The excellent agreement between theory and experiment should be noted. The normalized total Raman emission and the transmitted laser light do not add up to unity, because of linear losses of the system and the energy transfer to molecular vibrations.

We have measured the backward-scattered Raman power for pulses with $T \simeq 0.6$ nsec. The ratio of backward to forward Raman power was less than 10^{-2}; this observation is not surprising, since the gain of the backward-travelling Raman pulse is seriously limited by an effective length of approximately $cT/2n \simeq 5$ cm; the forward-emitted Raman light is amplified over the full length of the cell of 30 cm.[22]

F. FIRST- AND SECOND-ORDER STOKES RADIATION

For a better understanding of the stimulated Raman process, and for a more detailed comparison with theory, the first- and second-order Stokes radiation were investigated simultaneously as a function of the incident laser power. The experimental system is depicted in Fig. 7.

It was first ascertained by photographic techniques that the Raman emission occurred as well defined frequencies, which were Stokes shifted from the incident ruby line $\tilde{\nu}_L = 14,400$ cm^{-1} by multiples of 656 cm^{-1}. It should be emphasized that our spectral pattern is completely different from the broad, rather continuous Raman emission observed in small scale filaments.[23] As pointed out above, in our system the Raman emission occurs over the whole cross section of the incident laser beam.

For a quantitative investigation of the emission power of the first and second Stokes component P_{S1} and P_{S2}, two fast photodetectors were placed behind a three-prism spectrometer (25 A/mm).

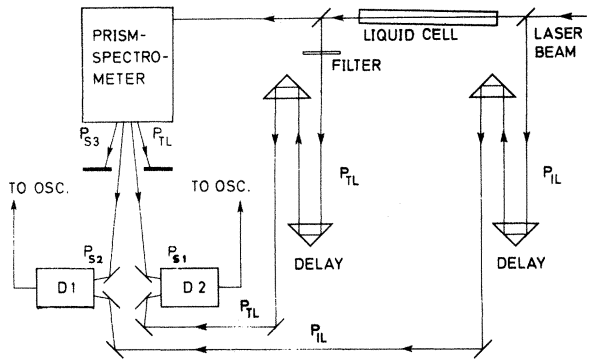

FIG. 7. Schematic setup for measuring first- and second-order Stokes power. Second-order Stokes and incident laser light are recorded by photodetector D1; first-order Stokes and transmitted laser light are recorded by photodetector D2.

The positions of the photodetectors were adjusted according to the line spectra obtained on photographic plates. Each of the photodetectors measured, in addition, a second pulse train, P_{IL} or P_{TL}, both being optically delayed by approximately 4 nsec. After properly calibrating the spectrometer, the ratios P_{S1}/P_{IL}, P_{S2}/P_{IL}, and P_{TL}/P_{IL} were determined and plotted as a function of the incident peak laser intensity $I_L(0,0)$.

A typical result is presented in Fig. 8 for $T=0.6$ nsec. The three curves are calculated with $g_0=10^{-2}$ cm/MW, $z_0=30$ cm, and $\alpha_0=3\times10^{-3}$ cm^{-1}; they are equivalent to those of Fig. 2. There is remarkable agreement between the theoretical curves and our experimental points. For different pulse trains, there were some variations in the onset of the second Stokes emission; the early appearance of P_{S2} is believed to be caused by some light filaments.

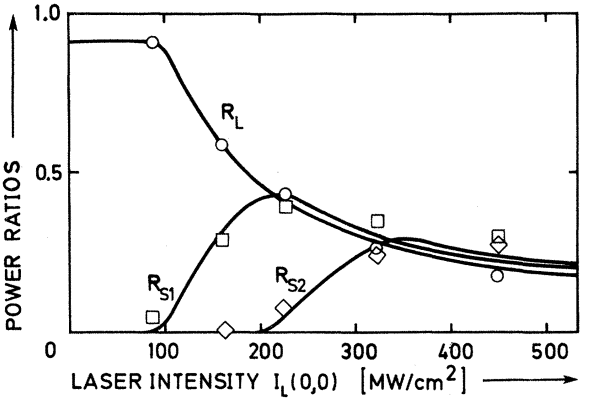

FIG. 8. Normalized transmitted laser (R_L), first (R_{S1}) and second Stokes (R_{S2}) power as a function of the incident laser intensity $I_L(0,0)$. The circles, rectangles, and diamonds represent the experimental values of R_L, R_{S1}, and R_{S2}, respectively. The solid curves are calculated according to the theory discussed in the text.

G. DISCUSSION

In the preceding sections, we have presented experimental observations of the stimulated Raman effect obtained with light pulses of 0.6 nsec duration. The application of these short pulses has several advantages.

(a) The pulse duration is short compared to the acoustic phonon lifetime of CS_2 of $\tau_B=2.5$ nsec[13,24]; as a result, the conditions for stimulated Brillouin scattering are far from the steady-state situation. In fact, SBS has not been observed with these short pulses. Competing and disturbing effects due to SBS are eliminated in our investigations.

(b) The pulse duration is long compared to the Raman time constant $\tau_R=1/(2\pi c\,\Delta\tilde{\nu})\simeq10^{-11}$ sec, i.e., we can compare our results with a steady-state theory, using the known gain coefficient for stimulated Raman scattering.

(c) Short pulses are available at high-peak intensities. In our experiments, peak power values of close to 20 MW and peak intensities approaching 10^3 MW/cm^2 were used. With these pulses, we worked far in the saturation range of SRS with high gain over the total beam cross section. In this way, the effect of individual filaments was essentially eliminated.

(d) At the high laser intensities, collimated beams could be used which made a quantitative comparison with theory possible. The small beam angle avoided the generation of significant amounts of anti-Stokes and off-axis Stokes radiation.

Some words should be said why CS_2 was chosen in our investigations.

The reason for selecting CS_2 is twofold. CS_2 has a long acoustic-phonon lifetime τ_B, and a high gain coefficient for stimulated Raman scattering. Both properties are important for a quantitative analysis as discussed above under points (a) and (c). To emphasize this fact, some preliminary results with CCl_4 ($\tau_B=0.25$ nsec and $g_{SRS}=3.5\times10^{-4}$ cm/MW) should be reported. With the same short pulses, we found substantial conversion of laser into Raman light ($P_R/P_{IL}\simeq30\%$); but the appearance of SBS ($\simeq20\%$) made a quantitative comparison with theory very difficult. It is obvious that still shorter light pulses are required for the investigation of this material.

In Fig. 8, the intensity dependence of the transmitted laser light and the first and second Stokes components agreed well with theoretical predictions for a Gaussian laser beam. In particular, the high conversion efficiencies and the strong monotonic decrease of the transmitted laser light with increasing incident intensity were well established. In addition, the successive maxima of the various Stokes components are clearly seen in Fig. 8. It should be noted that the emission of the different Stokes components depends very strongly upon the incident laser intensity and the length of the amplifying medium. As an example, the power ratios at a definite laser intensity will be discussed. For $I_L(0,0)=320$ MW/cm^2 and $z_0=30$ cm, the transmitted laser power R_L and the first and second Stokes emission R_{S1} and R_{S2} are of approximately equal value ($\simeq30\%$), while the third and fourth Stokes component is

smaller by a factor of 10^4 and 10^{12}, respectively. It can be stated more generally that at high incident laser intensities, the lower Stokes components are of approximately equal intensity, while the higher Stokes waves have rapidly decreasing intensity values.

In conclusion, we wish to say that the theoretically predicted high Raman conversion efficiency has been confirmed experimentally. The good agreement between theory and experiment allows the determination of steady-state gain coefficients in substances where this value is still unknown.

ACKNOWLEDGMENT

The authors are indebted to O. Rahn for valuable experimental assistance during the later part of this work.

---

[1]For a summary see N. Bloembergen, Am. J. Phys. 35, 989 (1967).

[2]R. G. Brewer, Phys. Letters 11, 294 (1964); P. Lallemand and N. Bloembergen, Appl. Phys. Letters 6, 210 (1965); D. Weiner, S. E. Schwarz, and F. J. McClung, J. Appl. Phys. 36, 2395 (1965); G. Bret and G. Mayer, in Physics of Quantum Electronics, edited by P. Kelley, B. Lax, and P. Tannenwald (McGraw-Hill Book Co. Inc., New York, 1966).

[3]E. Garmire, F. Pandarese, and C. H. Townes, Phys. Rev. Letters 11, 160 (1963).

[4]Y. R. Shen and N. Bloembergen, Phys. Rev. 137A, 1787 (1965).

[5]Y. R. Shen and Y. J. Shaham, Phys. Rev. Letters 15, 1008 (1965); P. Lallemand and N. Bloembergen, *ibid.* 15, 1010 (1965); G. Hauchecorne and G. Mayer, Compt. Rend. 261, 4014 (1965); Y. R. Shen and Y. J. Shaham, Phys. Rev. 163, 224 (1967).

[6]E. Garmire and C. H. Townes, Appl. Phys. Letters 5, 84 (1964); T. Ito and H. Takuma, in Physics of Quantum Electronics, edited by P. Kelley, B. Lax, and P. Tannenwald (McGraw-Hill Book Co. Inc., New York, 1966); S. E. Schwarz and A. Pine, Appl. Phys. Letters 9, 49 (1966).

[7]E. Garmire, R. Y. Chiao, and C. H. Townes, Phys. Rev. Letters 16, 347 (1966); C. C. Wang and G. W. Racette, Appl. Phys. Letters 8, 256 (1966).

[8]M. Maier, W. Kaiser, and J. A. Giordmaine, Phys. Rev. Letters 17, 1275 (1966), and Phys. Rev. 177, 580 (1969).

[9]N. Bloembergen, P. Lallemand, and A. Pine, IEEE J. Quant. Electr. 2, 246 (1966).

[10]R. G. Brewer, J. R. Lifshitz, E. Garmire, R. Y. Chiao, and C. H. Townes, Phys. Rev. 166, 326 (1968); D. H. Close, C. R. Giuliano, R. W. Hellwarth, L. D. Hess, F. J. McClung, and W. G. Wagner, IEEE J. Quant. Electr. 2, 553 (1966).

[11]J. Walder and C. L. Tang, Phys. Rev. 155, 318 (1967).

[12]M. Maier, Phys. Rev. 166, 113 (1968).

[13]D. Pohl, M. Maier, and W. Kaiser, Phys. Rev. Letters 20, 366 (1968).

[14]M. Denariez and G. Bret, Phys. Rev. 171, 160 (1968).

[15]N. M. Kroll, J. Appl. Phys. 36, 34 (1965).

[16]S. L. Shapiro, J. A. Giordmaine, and K. W. Wecht, Phys. Rev. Letters 19, 1093 (1967); G. Bret and H. P. Weber, to be published.

[17]J. G. Skinner and W. G. Nilsen, J. Opt. Soc. Amer. 58, 113 (1968).

[18]W. R. Clements and B. P. Stoicheff, Appl. Phys. Letters 12, 246 (1968).

[19]The values of $P_L(0)$ and $P_L(z_0)$ are identical with the experimental quantities P_{IL} and P_{TL}, the incident and transmitted laser power, respectively.

[20]R. W. Mocker and R. J. Collins, Appl. Phys. Letters 7, 270 (1966); A. J. DeMaria, D. A. Stetser, and H. Heynan, Appl. Phys. Letters 8, 174 (1966).

[21]Two-photon absorption is not important in CS_2. M. Maier, W. Rother, and W. Kaiser, Phys. Letters 23, 83 (1966).

[22]It should be noted that the short length of the light pulse also reduces the gain for SBS.

[23]R. G. Brewer, Phys. Rev. Letters 19, 8 (1967); H. P. H. Grieneisen and C. A. Sacchi, Bull. Am. Phys. Soc. 12, 686 (1967); F. Shimizu, Phys. Rev. Letters 19, 1097 (1967); A. C. Cheung, D. M. Rank, R. Y. Chiao, and C. H. Townes, *ibid.* 20, 787 (1968).

[24]P. A. Fleury and R. Y. Chiao, J. Acoust. Soc. Am. 39, 751 (1966).